Forensic Science International 382 (2026) 112871

Contents lists available at ScienceDirect

Forensic Science International

journal homepage: www.elsevier.com/locate/forsciint

Stable isotopes (δ13C, δ15N, δ34S) of human skin during decomposition

Ryan Pawlowski [a,*], Shari L. Forbes [b], Paul Szpak [a]

[a] Department of Anthropology, Trent University, 1600 W Bank Dr, Peterborough, ON K9L 0G2, Canada
[b] Department of Chemistry and Biochemistry, University of Windsor, Sunset Avenue, Windsor, ON N9B 3P4, Canada

ARTICLE INFO

Keywords:
Stable Isotope Analysis
Forensic Science
Postmortem Interval
Decomposition
Carbon
Nitrogen
Sulfur

ABSTRACT

In forensic investigations, estimation of the postmortem interval, or time since death, is essential to the legal process. The timeline of decomposition can be estimated through the use of various methods, however, these methods become less accurate or applicable in later stages. Previous stable isotope studies identify skin as a potentially useful substrate in the context of decomposition due to its durable nature, with some tissues exhibiting an increase in $\delta^{15}N$ over time. In this study, stable isotope analysis was performed on human skin samples, collected from donors over several months within a "body farm" human decomposition facility. Changes in $\delta^{13}C$, $\delta^{15}N$, and $\delta^{34}S$, and the impacts of sample pretreatments (chemical lipid extraction and protein solubilization) were examined in a 2 × 2 factorial design to determine the optimal sample pre-treatments to observe decomposition-associated changes. Through examination of interactions between decomposition byproducts and chemical pretreatments, our research was able to identify relationships between temperature, decay state, and isotopic changes. Our findings suggest that while changes occur in $\delta^{13}C$ and $\delta^{15}N$ in bulk skin during decomposition, the isolation of individual organic compounds may provide a better means of measuring and observing decomposition-driven isotopic changes relative to isotopic analysis of bulk skin and, therefore, represent a more promising avenue of research for estimating postmortem interval.

1. Introduction

Upon the discovery of human remains, several unknowns arise regarding the context and nature of the deceased, requiring the expertise of forensic scientists. Using a variety of interpretive techniques, forensic anthropologists and pathologists assess the state of remains to estimate the postmortem interval (PMI), or time since death [1]. Early assessments can be reliably made through PMI methods such as stimulation of the muscles and eyes, vitreous potassium eye content, and simple visual identification of the transitional mortis stages [2–4]. As putrefaction marks the transition from early to late PMI determination, assessment becomes increasingly difficult [5]. Environmental variables of temperature, moisture, location, and exposure are known to impact the progression and intensity of decomposition processes, therefore decreasing the accuracy of PMI determination [6–8]. Among late PMI methods, forensic entomology is currently regarded as the best means of interpreting decomposition, identifying cycles of certain insects as coinciding with stages of decay [9]. While reliable, assessments using forensic entomology are unable to be applied in certain contexts, such as in obstructive burial environments or with skeletonized remains [7]. Therefore, no singular "best" method currently exists to assess PMI for both early and advanced decay stages. This poses a significant challenge for forensic investigations, where remains are often found heavily decomposed, lacking significant soft tissue, or skeletonized [8,10,11]. Therefore, exploration of new avenues of PMI estimation is vital for building our understanding of decomposition, to compensate for situations where other methods fall short.

Applied to hard and soft tissues, stable isotope analysis has found success in forensic science, aiding in the identification of victims of homicide and humanitarian conflicts using $\delta^{2}H$, $\delta^{13}C$, $\delta^{15}N$, $\delta^{18}O$, and $\delta^{34}S$, as well as strontium ($^{87}Sr/\ ^{86}Sr$) and lead (^{204}Pb, ^{206}Pb, ^{207}Pb, ^{208}Pb) isotope systems [12–16]. The substrate of skin is particularly underutilized in stable isotope research, especially in the forensic context. Comprised of durable keratinocytes, elastin, and several types of collagen within the dermal layers, skin is the first line of defense against environmental contact and trauma [17]. Keratin and collagen are highly resistant to processes of enzymatic and microbial breakdown that occur during decomposition [18,19]. Strong molecular forces associated with the triple helical structure of collagen and disulfide bonds of keratin allow skin to endure decomposition for months to

* Correspondence to: 1600 W Bank Dr, Peterborough, ON K9L 0G2, Canada.
E-mail address: Ryanpawlowski@trentu.ca (R. Pawlowski).

https://doi.org/10.1016/j.forsciint.2026.112871
Received 16 November 2025; Received in revised form 2 February 2026; Accepted 4 February 2026
Available online 5 February 2026

years, well beyond the degradation of muscles, and organs, such as the brain, liver and kidneys [18,19]. While the durability and availability of bone surpasses that of skin in a decomposition context, skin offers a promising middle ground between soft and hard tissues for PMI estimation. Surviving well into decomposition when desiccated while still exhibiting decomposition-associated changes, skin's durability and overall abundance identify it as a reliably procurable sampling material for forensic purposes.

While not all aspects of isotopic variability of skin are understood, skin is tentatively regarded as an isotopically homogenous material, displaying a similar stable isotope composition regardless of sampling location following lipid extraction [20–23]. From basal layer to epidermis, the cycle of human epidermal tissue displays a short average turnover time of 40–56 days [24,25]. The stable isotope compositions of collagen extracted from skin will therefore reflect weeks to months of life history [26]. The combination of durability, short turnover, and widespread homogeneity further identifies skin as an ideal substrate for forensic purposes, with any skin sample providing stable isotope compositions representative of a relatively short period of time before death. However, as remains of forensic significance are rarely identified prior to decomposition, considerations must be made regarding how decomposition interreacts with isotopic and elemental compositions.

The impact of decomposition on the $\delta^{13}C$, $\delta^{15}N$, and $\delta^{34}S$ of organic tissues is not well established. Current studies of soft tissue decomposition have been applied primarily to marine fauna, such as cetaceans, pinnipeds and fish [27–30]. Stranded or beached animals are a common sampling source in marine studies, due to laws restricting access to marine mammals for research purposes [30,31]. Under various periods of decay, marine studies identified variable enrichment of ^{15}N and limited depletion of ^{13}C present in decomposition context tissues [27,28], [229], [30]. Examinations of mammalian and human soft tissues identify more substantial increases in $\delta^{15}N$, reaching 1–3 ‰ above initial values in both beaver and human muscle tissue [32,33]. A recent outdoor decomposition study in Texas by Miles [34] identified an increase of 2.5 ‰ in $\delta^{15}N$ values of lipid-extracted human muscle tissue within 10 days of environmental exposure [34]. While no significant changes were identified in human skin $\delta^{13}C$ or $\delta^{15}N$, this research currently provides the only examination of human skin in a postmortem context. Therefore, there is inherent value to further examining decomposition-related change in skin, while also growing our understanding of the relationship between decomposition and isotopic alterations.

Across all animal-based, and most human-based decomposition studies, tissue samples were not subjected to any form of chemical pretreatment prior to isotopic analysis, with some research specifying the lack of treatment as a means to preserve products of decomposition [32,33]. While abstaining from these pretreatments produces the most "natural" sample, the variable retention of lipids, contaminants, and non-collagenous proteins likely obscures temporal variation in $\delta^{13}C$ and $\delta^{15}N$ associated with decomposition [35–37]. By preserving the heterogeneity of the sample, interpreting decomposition and its interactions with these variable components becomes exponentially more difficult. Additionally, liquid putrefaction products have been found to adhere to skin [38,39]. As decomposition fluids are known to display increased $\delta^{15}N$ values in comparison to bulk body tissues, the lack of treatment may unevenly preserve the putrefaction byproducts of skin, likely introducing further isotopic variability in untreated samples [40]. While skin is not completely resistant to decomposition, it is likely that these fluids are not representative of skin and are instead representative of other previously autolyzed tissues. Accordingly, we employed different pretreatment protocols to the same skin sample to assess changes in the isotopic composition of skin.

Miles [34] was the first isotope-focused decomposition study to include a chemical pretreatment step, where human muscle and skin was subjected to chemical lipid extraction using a 2:1 chloroform methanol solution [41]. A common pretreatment practice in stable isotope analysis of animal tissues, lipid extraction removes lipids that are depleted in ^{13}C relative to the substrate, increasing the homogeneity of the sample and stable isotope values [42]. The combination of lipid extraction with collagen solubilization (refluxing), which removes non collagenous proteins and humic contaminants, is regularly used to produce highly homogenous collagen extracts from bone [35,43]. Due to the inclusion of the lipid extraction step, the isotopic findings of Miles [31] are not representative of a heterogeneous, natural sample, but of a more homogenous sample with some components removed. It is not currently known how pretreated, homogenized samples compare to untreated samples, or how different pretreatments interact with byproducts produced from decomposition.

In this research, we hypothesized that stable isotope analysis of $\delta^{13}C$, $\delta^{15}N$, and $\delta^{34}S$ applied to decomposition context human skin can provide a means to estimate postmortem interval. We propose that the isotopic analysis of different fractions of a skin sample, subjected to variable pretreatment combinations of lipid extraction and refluxing (solubilization), will isolate different compounds, allowing for more precise examination of decomposition-associated alterations. Through different pretreatments, we aim to identify, then interpret, the degree of isotopic alteration over the decomposition timeline, for the benefit of both forensic and ecological stable isotope work.

2. Methods

Skin samples were collected from elderly human donors placed within the REST[ES] (Research in Experimental and Social Thanatology) body facility. Located in Quebec, Canada and operated by Université du Québec à Trois-Rivières (UQTR), the REST[ES] facility is remotely situated within a temperate forest/wetland environment comprised of white pine, red maple, and white spruce trees, with minimal incline [44]. Secure fencing paired with galvanized mesh cages placed atop donor individuals deter scavenging, while providing unobscured environmental exposure to the cold climate conditions, including sub-zero winter temperatures [44,45].

The population of donors placed within REST[ES] is exclusively comprised of individuals who have expressed explicit consent to participation through UQTR's body donation program [44]. Donor identities have been numerically anonymized for privacy, with information relating to aspects of life, medical history, and death provided in Table S1. All donors sampled for this study died of natural causes and featured no physical trauma as to not alter decomposition processes.

Skin samples were collected from $n = 4$ individuals placed within the REST[ES] facility. Donor sampling commenced May 4th, 2023, and concluded April 13th, 2024, for a period of 345 days. Placement occurred within 1–3 days postmortem. Upon entering the facility, donors were placed within designated areas in direct contact with the forest floor, with galvanized mesh cages placed over top, providing protection until contact is necessary. Skin samples were collected using disposable 8 mm biopsy punches or cut using a scalpel, yielding tissue samples ~1–3 cm in diameter/length. Samples were taken from the shoulder, the quadricep region of the thigh, or from any location with remaining tissue as decomposition progressed. Each donor was subjected to a uniform sampling schedule, featuring repeated sampling with less frequency over time. New donors were sampled every 2 days (± 1 day) for two weeks, producing a maximum of six samples during this period. A maximum of four samples were collected weekly or biweekly for one month, followed by monthly sampling afterwards. Sampling date, location and side were recorded, and samples were immediately stored at –20°C to prevent further decomposition. Under the outlined sampling procedure, $n = 35$ skin samples were collected from the four donors for this research.

Prior to treatment, skin samples were isolated from adhering fat and muscle tissue, removed via scalpel. Skin samples were cut into two halves – Segment 1 and Segment 2 – to allow for the application of different pretreatments. Segment 1 remained untreated (0/0), while Segment 2 was subjected to a chemical lipid extraction step (LE/0). Both

0/0 and LE/0 samples were later subjected to a refluxing step (R), to attempt to isolate the collagenous fraction of the skin, allowing for a 2 × 2 factorial design for the analyses with minimal sample consumption (Fig. 1).

The chemical lipid extraction step followed that described by Finucane et al. [47], which adapted the procedure of Folch et al. [41]. LE/0 samples were immersed in 7 mL of 2:1 chloroform:methanol solution in 13 × 100 mm glass culture tubes, sealed, and placed in an ultrasonic bath for 1 h. Samples were then removed from the bath, and the solution was replaced. The waste solution was transferred using Pasteur pipettes into a new 13 × 100 mm glass culture tube for future analysis. This process repeated for a total of three 1 h sonication cycles. By final sonication, lipids could no longer be visually identified within the waste solution. Samples were then left to evaporate at room temperature in a fume hood for 36 h. The 0/0 and LE/0 samples were freeze-dried and weighed into tin caps for stable isotope analysis.

Following sampling, both 0/0 and LE/0 samples were subjected to refluxing, becoming the 0/R and LE/R treatments, respectively. Skin samples were submerged in 3.5 mL of 0.01 M HCl and placed in an oven at 65°C for 36 h. This procedure breaks down the hydrogen bonds that hold together the three strains of the collagen triple helix, rendering the collagen water-soluble. The refluxed collagen was then transferred using Pasteur pipettes into pre-weighed 4 mL glass vials, which were subsequently frozen and lyophilized. After the treatments were concluded, samples were weighed into tin caps for stable isotope and elemental analysis.

Stable isotope and elemental analysis was performed using two different elemental analyzer-isotope ratio mass spectrometer (EA-IRMS) systems: an Elementar Vario ISOTOPE Cube EA coupled to an Isoprime visION IRMS, and a Nu Horizon IRMS coupled to a EuroVector EA 3000 elemental analyzer, both housed in and operated by Trent University's Water Quality Centre (Peterborough, ON, Canada). The Cube system provided the means to analyse stable carbon, nitrogen and sulfur (CNS) isotope values with a purge trap EA system [48], while the Nu Horizon allowed for the analysis of stable carbon and nitrogen (CN) isotopes with a traditional EA equipped with a GC column. Sample duplicates were produced every 10th sample to examine precision.

Following sample preparation and pretreatment, sample mass was significantly reduced by the removal of lipids during lipid extraction (LE), the evaporation of 2:1 chloroform methanol and water following lipid extraction, and reduced further following the removal of water via lyophilization (freeze drying). Following lipid extraction and freeze-drying processes, sample mass was found to be reduced by approximately 66–83 % in comparison to initial values, as identified by interquartile range, yielding samples as small as 1.7 mg. Some small samples were therefore excluded from CNS analysis using the Elementar Cube due to their size being insufficient for sampling prior to refluxing. As such, δ^{34}S values were only able to be analyzed for 0/0 and LE/0 samples weighing 6 mg or above, as this would yield sufficient sulfur for accurate analysis. All samples with a total mass below 6 mg were only analyzed on the EuroVector/Nu Horizon EA-IRMS for δ^{13}C and δ^{15}N (not δ^{34}S).

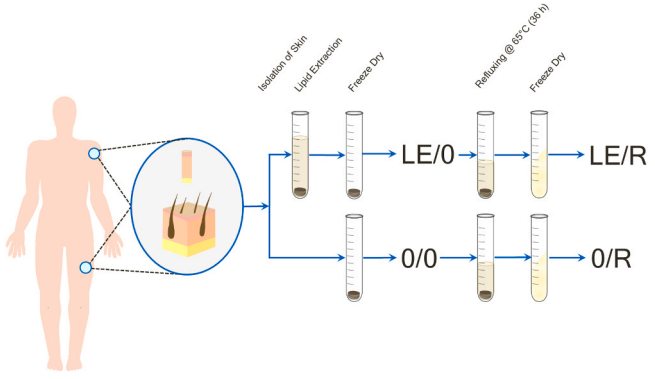

Fig. 1. Schematic displaying different pretreatments applied to the skin samples (after Szpak et al. [46]).

Stable carbon, nitrogen and sulfur isotopic compositions were calibrated relative to the Vienna Pee Dee Belemnite (VPDB), Atmospheric Inhalable Reservoir (AIR), and Vienna-Canyon Diablo Troilite (VCDT) scales using a multi-point normalization (Table 1). Two international and seven in-house reference materials were used as quality control (QC) standards to monitor measurement uncertainty.

Precision (*u(Rw)*) calculations indicated analytical precision to be ± 0.15 ‰ for δ^{13}C, ± 0.21 ‰ for δ^{15}N, and ± 0.38 ‰ for δ^{34}S based on repeated measurements of calibration standards, QC standards, and sample replicates. Systematic error (*u(bias)*), calculated by comparing the observed and known values of the standards, was found to be ± 0.16 ‰ for δ^{13}C, ± 0.19 ‰ for δ^{15}N, and ± 0.45 ‰ for δ^{34}S. Calculations identified an analytic uncertainty (u_c) of ± 0.23 ‰ for δ^{13}C, ± 0.28 ‰ for δ^{15}N, and ± 0.6 ‰ for δ^{34}S, reported in accordance with Szpak [49].

Elemental compositions were discussed using atomic C:N ratios (C:N_{Atomic}), where C:N_{Atomic} ratios are defined as a ratio of carbon to nitrogen atoms in a compound, rather than the ratio of mass used in molecular C:N ratios. To illustrate this difference, the C:N_{Atomic} ratio of caffeine ($C_8H_{10}N_4O_2$) would be 8:4 or 2, while the C:$N_{Molecular}$ ratio of caffeine would be 1.71 or (8 ×12.011)× (4 ×14.007)$^{-1}$ [34]. All mentions of C:N or C:N ratio refer to the atomic C:N ratio, as defined in this section.

Due to the limited sampling collected for Donor 24, comparative

Table 1
International (USGS and IAEA) and in-house reference materials used as calibration or quality control reference materials.

Reference Material	Description of Material	Reference Material Type	$\delta^{13}C_{VPBD}$ (‰)	$\delta^{15}N_{AIR}$ (‰)	$\delta^{34}S_{VCDT}$ (‰)
IAEA-CH-7	Polyethylene	Calibration	–32.15 ± 0.05	-	-
IAEA-S-1	Silver sulfide	Calibration	-	-	–0.30 ± 0.00
IAEA-S-2	Silver sulfide	Calibration	-	-	22.62 ± 0.1
IAEA-S-3	Silver sulfide	Calibration	-	-	–32.47 ± 0.1
USGS25	Ammonium sulfate	Calibration	-	–30.41 ± 0.27	-
USGS40	Glutamic acid	Calibration	–26.39 ± 0.04	–4.52 ± 0.06	-
USGS41a	Glutamic acid	Calibration	36.55 ± 0.08	47.55 ± 0.15	-
USGS62	Caffeine	Calibration	–14.79 ± 0.04	20.17 ± 0.06	-
USGS63	Caffeine	Calibration	–1.17 ± 0.04	37.83 ± 0.06	-
SRM-7	Albendazole	Calibration	-	-	–14.69 ± 0.5
USGS88	Marine fish collagen	QC	-	-	17.28 ± 0.3
USGS89	Porcine collagen	QC	-	-	3.67 ± 0.2
SRM-1	Caribou bone collagen	QC	–19.36 ± 0.06	1.90 ± 0.14	-
SRM-4	Wheat gluten	QC	–26.93 ± 0.29	5.23 ± 0.17	–6.78 ± 0.1
SRM-8	Amoxicillin	QC	-	-	5.87 ± 0.3
SRM-9	Ram horn	QC	-	-	2.32 ± 0.3
SRM-10	Beef protein	QC	–14.48 ± 0.03	6.40 ± 0.07	-
SRM-14	Polar bear bone collagen	QC	–13.62 ± 0.07	21.67 ± 0.14	-
SRM-26	Marine collagen	QC	–16.23 ± 0.17	14.69 ± 0.13	16.90 ± 0.6

analysis of donors was performed only using values generated from Donors 22, 23, and 25. For treatment-to-treatment comparisons, all donor values, including Donor 24, were incorporated as combined results. All results for one sample (27934) were excluded from statistical consideration for displaying isotopic values, elemental values, and C:N ratios not representative of collagen or human skin. Two stable isotope measurements were also removed: one untreated value was excluded for exhibiting an extreme C:N ratio of 148.3, indicative of an instrumental error, and one 0/R value for exhibiting an anomalously low C:N ratio of 2.79, similar to the excluded sample.

A Shapiro-Wilk test was applied to all isotopic and elemental compositions, as well as measures of accumulated degree days (ADD), to assess normality. Kruskal-Wallis and Dunn's post-hoc tests were applied to all comparisons to account for non-normal distributions of data and the variable nature of decomposition. Spearman's *rho* was used to assess relationships between ADD and stable isotopic values. Statistical analysis and LOESS regression analysis was performed using PAST version 5.2.2 [50].

3. Results

3.1. Accumulated degree days (ADD), weather data and total body scoring

All averaged weather data is presented in Table S3. Visualization of minimum, maximum and average temperatures of the sampling period is presented in Fig. 2, with additional notation for donor tissue retention. Within the northern continental environment, the average temperature of the sampling period was found to be 7.64 ± 9.91°C. Summer temperatures reached as high as 34.6°C, while winter temperatures reached as low as −21.6°C. Minimum and maximum temperatures were found to fluctuate by as much as 24.3°C, or as little as 1.1°C within a 24-hour period, for an average difference of 8.95°C. Median precipitation of the sampling period was found to be 0.2 mm. 81 days of the sampling period featured no rainfall, while an additional 45 days had no data recorded. Relative humidity of the sampling period was an average of 79.4 ± 13.8 %, reaching a maximum of 100 % (October 9th 2023) and minimum of 41.7 % (May 7th, 2023).

Of the four examined individuals, Donors 22 and 23 were subjected to climbing summer temperatures, while Donors 23, 24 and 25 were exposed to freezing temperatures and winter conditions. Accumulated degree days (ADD) were calculated for each donor to model the relationship between temperature and decomposition progress [51]. To calculate ADD, the average daily temperature was progressively recorded and summed for each donor, commencing upon entry and concluding upon total skeletonization or removal [51]. Total accumulated degree days reached a minimum of 1176.8 ADD and a maximum of 2506.3 ADD. Average temperatures ≤ 0°C were found to occur for 88 days of the 345-day period, resulting in no change in ADD [51]. Total body scoring (TBS) following Megyesi et al.'s [51] guided assessment of decomposition milestones and progress over time (Fig. 3). First instances of bloat occurred within 4–29 days postmortem (16–382 ADD) in Donors 22, 24 and 25, while no bloat was identified in Donor 23. The active decay stage was identified within 9–11 days postmortem (126 and 172 ADD). Donor 22 was the only donor to achieve skeletonization, identified as occurring between 97 and 127 days postmortem, with other donors remaining in an advanced decomposition state by the end of the sampling period.

3.2. Untreated skin stable isotope values

All isotopic and elemental compositions are presented in full in Table S2. Stable isotope analysis of untreated skin produced $\delta^{13}C$ values ranging from −23.91 ‰ to −19.43 ‰, with an average $\delta^{13}C$ value of −21.95 ‰. Changes in untreated sample $\delta^{13}C$ values displayed no trends of subsequent increase or decrease throughout the sampling timeline. Regardless of deposition date and associated environmental exposure, a Kruskal-Wallis test identified no significant differences among untreated donor $\delta^{13}C$ values ($H[3] = 2.28, p = 0.52$). Untreated samples displayed an average atomic C:N ratio of 7.24 ± 3.73. While no subsequent changes in C:N ratio were identified over time, C:N ratios ranged between 3.44 and 19.81, indicating extreme variability in untreated sample elemental composition independent of decomposition.

Skin $\delta^{15}N$ was found to increase over time as a function of TBS assessment. Maximum $\delta^{15}N$ values of 0/0 skin were found to occur during the active decomposition stage. Average values displayed a range of + 10.61 ‰ to + 17.62 ‰, with progressive increases reaching + 1.50 ‰ to + 5.02 ‰ above initial donor $\delta^{15}N$ values. Upon reaching the maximum $\delta^{15}N$ value, donor values were found to decrease by 0.77 ‰ to 2.17 ‰ within the following period of 97–127 days, consistent across all examined individuals. Marginal significant differences ($H[3] = 7.3, p = 0.06$) were identified among untreated donor $\delta^{15}N$ values. Of the examined donors, significant differences were identified between Donor 22 and Donor 25 ($z = 2.66, p = 0.007$), who represent the earliest and latest summer depositions in the outdoor environment. A very strong positive correlation ($rho\ (10) = 0.93, p < 0.001$) was identified in Donor 22 between ADD and $\delta^{15}N$, while no correlation was identified between ADD and $\delta^{15}N$ in Donor 25. These findings suggest that

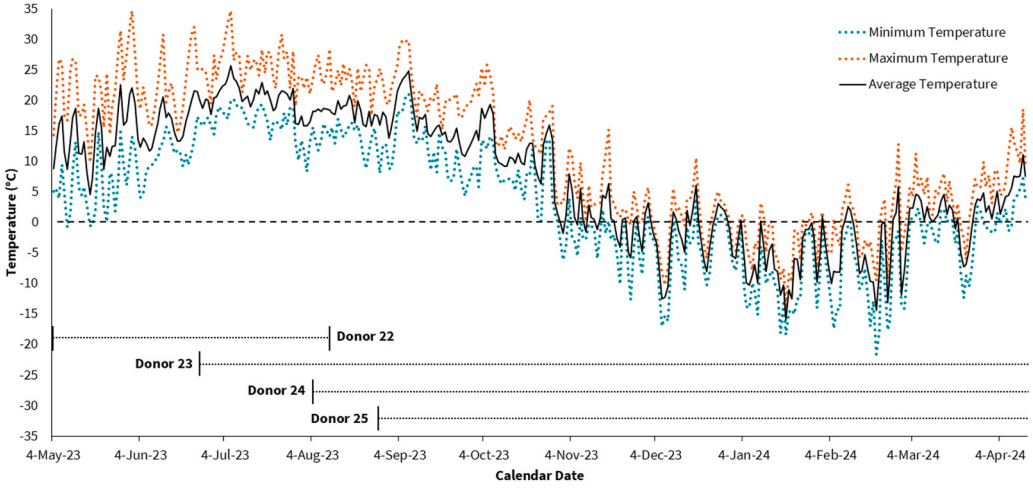

Fig. 2. Visualization of temperature variation and duration of donor environmental exposure for remains placed within the RESTES body farm environment, $n = 4$ individuals.

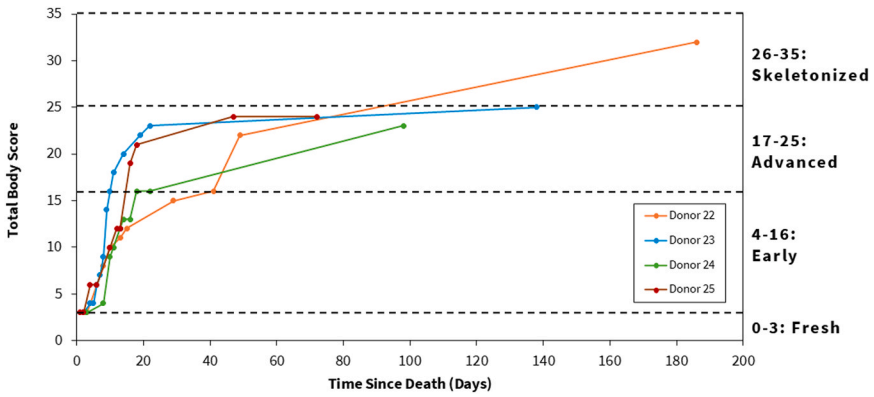

Fig. 3. Total body scoring following Megyesi *et al.* [51] reveals variation in donor-specific decomposition progression. Donor 22 achieved skeletonization, while other donors remained in an advanced decompositions state.

increases in δ^{15}N may be tied to higher temperatures that facilitate rapid decomposition.

3.3. Impacts of lipid extraction and refluxing treatments on $\delta^{13}C$

The application of chemical pretreatments was found to significantly impact the clarity of changes in δ^{13}C associated with decomposition. δ^{13}C values were found to significantly differ among treatments (Donor 22: $H[3] = 30.11$, Donor 23: $H[3] = 19.87$, Donor 25: $H[3] = 22.04$; $p < 0.001$ for all comparisons). Untreated skin samples were found to differ significantly from values generated under any form of pretreatment (Tables S4-S6), exhibiting δ^{13}C values lower than any of the pretreated skin. Comparison of δ^{13}C values of the same skin sample indicated that untreated skin samples displayed values as much as 6.65 ‰ lower than those of their LE/R counterparts. No significant differences were observed among the δ^{13}C values of different treatment combinations, identifying that the application of either or both lipid extraction and refluxing reduces variability in δ^{13}C values to a similar degree.

Examination of combined donor δ^{13}C values across treatments identified the combination of lipid extraction and refluxing as the best means of reducing the variability of δ^{13}C within samples (Table S7). Skin subjected to refluxing alone (0/R) was found to produce the most variable δ^{13}C values of all chemical treatments. Despite this, δ^{13}C values of refluxed skin were still found to be more comparable to values generated by LE/0 and LE/R samples, rather than those of untreated samples. Significant differences were found between donors under 0/R treatment ($H[3] = 13.57$, $p = 0.004$), where Donor 23 was found to significantly differ from all other individuals (Table S8). No differences were identified within other treatment groups, suggesting that refluxing alone may introduce some variability in δ^{13}C while removing depleted content.

3.4. Impacts of lipid extraction and refluxing treatments on $\delta^{15}N$

Combined donor δ^{15}N values indicate lipid extraction and refluxing as the best means of reducing variability in δ^{15}N caused by sample heterogeneity rather than decomposition, displaying the smallest mean value, range and standard deviation of all combined treatment values (Table S9). Refluxing alone generated the highest mean δ^{15}N, standard deviation and largest range of all sample δ^{15}N values, even surpassing untreated sample values. Across treatments, significant differences were identified in δ^{15}N values generated under LE/0 ($H[3] = 14.63$, $p = 0.002$) and LE/R ($H[3] = 22.53$, $p < 0.001$) treatments, with no significant differences identified among donors under 0/R (Table S10-S11). Both LE/0 and LE/R treatments identified δ^{15}N values of Donor 22 as significantly different from both Donor 23 and 25. As Donor 22 was subjected to the highest temperatures and experienced the most rapid decomposition, this suggests that lipid extraction may provide the best means to isolate and observe donor-specific substrate-bound changes in δ^{15}N.

Significant differences in δ^{15}N were identified between treatments for Donor 23 ($H[3] = 12.56$, $p = 0.006$) and Donor 25 ($H[3] = 18.44$, $p < 0.001$), with no differences identified in Donor 22. For Donor 23, δ^{15}N values of skin subjected to 0/R treatment were found to differ significantly from both LE/0 and LE/R treatments, with the addition of LE/R differing from untreated values (Table S12). Donor 25 identified 0/R values as differing significantly from all other treated and untreated values (Table S13). As the refluxing treatment was identified as different from other treatments in all donors, this suggests that refluxing alone does not uniformly impact δ^{15}N. Significant differences between 0/R and both refluxing treatments also suggest that 0/R does not reduce skin δ^{15}N variability as reliably as lipid extraction. Instead, refluxing may potentially introduce further variability in δ^{15}N, with values remaining close to or elevated above untreated δ^{15}N values.

3.5. LOESS regressions

LOESS regression (smoothing factor = 0.3) was applied to difference calculations for δ^{13}C, where Δ^{13}C represents the absolute difference between two delta (δ) values (in this case, the δ^{13}C of the earliest donor sample of each donor and each successive, associated δ^{13}C value) (Fig. 4). LOESS regression revealed slight trends of decrease in pretreated skin δ^{13}C values. Following a period of variability in the first ~300 ADD, a decrease in Δ^{13}C was observed over time in LE/0, 0/R and LE/R samples, occurring until 1709 ADD. 0/R samples generated the largest decrease over time, reaching approximately 1.5 ‰ below initial values, while LE/0 and LE/R samples displayed a decrease of less than 1 ‰. Untreated sample Δ^{13}C values were more variable than other treatments, requiring significantly more bootstrapping to account for sample heterogeneity. As such, trends of increase and decrease identified from untreated δ^{13}C values differ from those seen in chemically treated samples. LE/R treated skin displayed the smallest confidence intervals, and least variability of all tests.

LOESS regression (smoothing factor = 0.3) was applied to difference calculations for δ^{15}N, where Δ^{15}N represents the absolute difference between two delta (δ) values (in this case, the δ^{15}N of the earliest donor sample of each donor and one consecutive associated δ^{15}N value) (Fig. 5). LOESS regression analysis for δ^{15}N identified increases with ADD for all treatment samples. Within the first 300 ADD, δ^{15}N values for all skin increase. LE/0 and LE/R consistently display an increase in Δ^{15}N, reaching between 1 and 2 ‰ above the initial values by ~1700 ADD. Untreated and 0/R curves display stronger trends of increase, with values reaching up to 3 ‰ above initial values. Untreated and 0/R sample values also display more bootstrapping, indicating a wider spread of values and greater variability than lipid extraction-inclusive

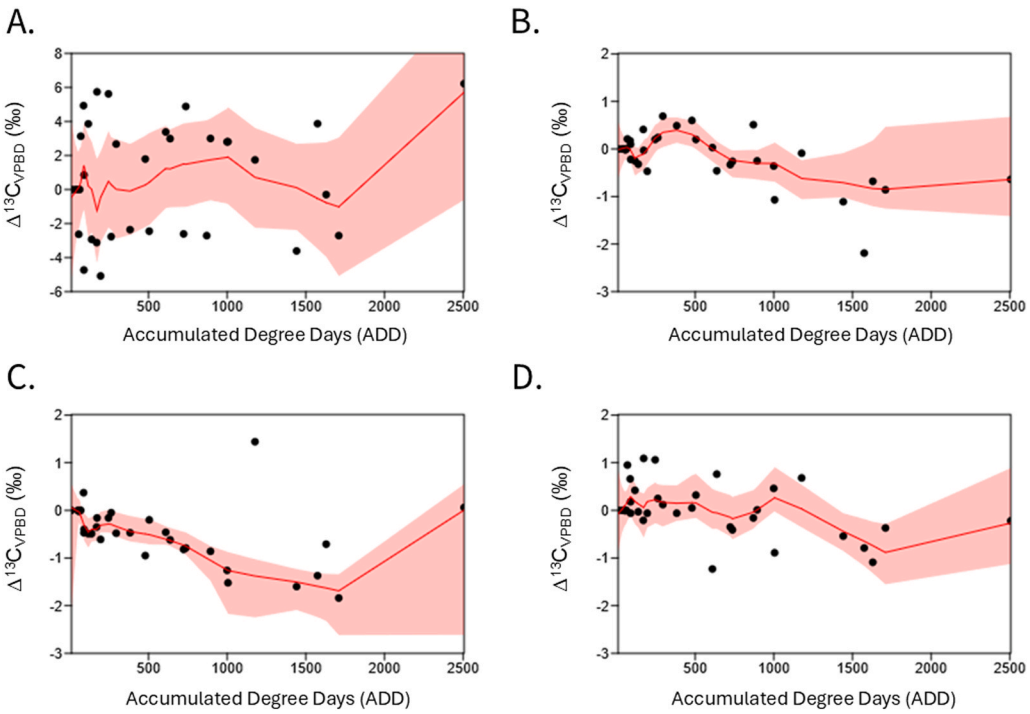

Fig. 4. LOESS regression reveals trends of decrease in $\Delta^{13}C$ ($\delta^{13}C_{Initial}$ - $\delta^{13}C_{Consecutive}$) as ADD increases. LE/R samples feature the least variability and lowest confidence intervals. A) 0/0. B) LE/0. C) 0/R. D) LE/R.

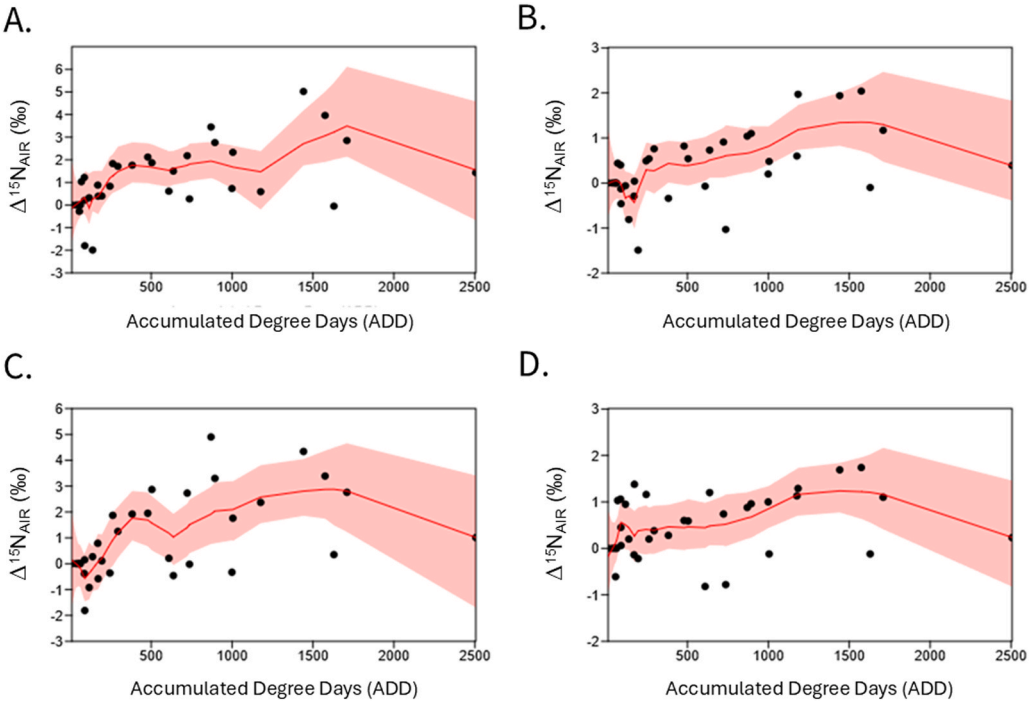

Fig. 5. LOESS regression displays trends of increase in $\Delta^{15}N$ ($\delta^{15}N_{Initial}$ - $\delta^{15}N_{Consecutive}$) as ADD increases. 0/0 and 0/R tests display a higher, more variable increase in $\delta^{15}N$, while LE/0 and LE/R display a lower but less variable increase. A) 0/0. B) LE/0. C) 0/R. D) LE/R.

treatments. The lack of variability suggests that chemical lipid extraction may dampen variability in $\delta^{15}N$, while still preserving the progressive increase in $\delta^{15}N$ over time.

3.6. Examination of $\delta^{34}S$ values of postmortem skin

Due to sample size requirements, the analysis of $\delta^{34}S$ was only possible for a portion of 0/0 and LE/0 samples. Significant differences in $\delta^{34}S$ were identified between donors for both untreated ($H[3] = 16.44$, $p < 0.001$) and LE/0 ($H[3] = 13.86$, $p = 0.003$) treatments. Untreated samples differed significantly for all donors, with the exception of Donor 25 displaying no differences relative to Donor 22 and 24 (Table S14-S15). LE/0 samples displayed significant differences between Donor 22 and Donors 24–25, while Donor 23 differed from Donor 24 alone.

Despite untreated and LE/0 samples displaying different significant differences, paired *t*-tests identified no significant differences between treatments, suggesting that the lipid extraction does not alter $\delta^{34}S$.

3.7. wt% C and wt% N

Untreated samples displayed the largest range, highest percentages, and highest standard deviation of wt% C, with a mean value of 53.2 %. Skin samples that underwent chemical pretreatment featured smaller ranges and lower standard deviation of wt% C. LE/0 skin featured the smallest wt% C range of 43.1–46.3 %, with measures varying by just 3.19 absolute percentage points. The 0/R and LE/R skin featured the lowest mean wt% C of all treatments, displaying mean values of 27.7 % and 27.8 %, respectively. Significant differences in wt% C were identified among pretreatments ($H[3] = 104.1$, $p < 0.001$), with differences occurring between all treatments but the pairing of 0/R and LE/R measures (Table S16). The refluxing step was found to cause the most significant change in wt% C, with 0/R and LE/R treated skin displaying lower wt% C measures of 23–33 %. No significant differences were observed between donor wt% C measures.

Significant differences ($H[3] = 76.47$, $p < 0.001$) were identified between wt% N measures generated under LE/0 versus all other treatments (Table S17). Samples treated under LE/0 resulted in the highest mean wt% N of 15.5 %, while also featuring the smallest range and standard deviation of all treatments. The 0/0, 0/R and LE/R samples were found to display similar mean measures of wt% N between 9.6 % and 9.9 %, suggesting the application of lipid extraction alters wt% N measures, which are then countered through the refluxing treatment. The 0/0 samples displayed the largest range of wt% N between 4.67 % and 14.11 %, while 0/R and LE/R treated samples displayed smaller ranges that were more comparable to LE/0 (13.09–16.72 %). 0/R and LE/R featured notably small ranges of wt% N, 8.19–11.26 % and 8.18–11.05 %, respectively, with LE/R displaying a slightly smaller range overall. No significant differences were observed between donor wt% N measures.

Untreated skin samples featured distinctly high C:N ratios in comparison to samples where any pretreatment had been applied (Fig. 6). In comparison to untreated samples, which displayed a C:N range between 3.44 and 19.5 and average of 7.24 ± 3.73, pretreated samples featured lower atomic C:N ratios, averaging to 3.38 ± 0.14 (LE/0), 3.24 ± 0.16 (0/R), and 3.30 ± 0.06 (LE/R).

Significant differences in combined donor data were identified between treatments ($H[3] = 80.5$, $p < 0.001$). Pretreated skin C:N ratios differed significantly from untreated C:N ratios, indicating that all pretreatments reduce variability in decomposition-context skin. Significant differences were also observed between C:N ratios of LE/0 and 0/R treatments. No differences were observed between LE/0 and LE/R, or 0/R and LE/R, suggesting that while lipid extraction reduces untreated skin C:N ratios in a different manner than refluxing, the difference is negligible when both are applied.

4. Discussion

Pretreatments of lipid extraction and refluxing were found to impact both $\delta^{13}C$ and $\delta^{15}N$. Untreated samples displayed significantly lower $\delta^{13}C$ values and high C:N ratios, indicative of high lipid content. All pretreatments were found to improve C:N ratio consistency and reduce "noise" likely caused by heterogenous components (e.g., lipids, non-collagenous proteins) within the samples, better visualizing trends of change related to decomposition. While no temporal trends were identified in untreated skin $\delta^{13}C$, there was a gradual decrease in $\delta^{13}C$ by 1–1.5 ‰ occurring 49–95 days after death for LE/0 and 0/R treatments (Fig. 4). In contrast, the increase in $\delta^{15}N$ values over time was attenuated during the LE/0 and LE/R treatments. The $\delta^{15}N$ values produced under LE/0 and LE/R were found to increase up to 2 ‰ above initial values, in comparison to the 1.5–5 ‰ seen in untreated samples, suggesting some removal of components with higher $\delta^{15}N$ alongside lipid content. Refluxing preserved increases in $\delta^{15}N$ that were visible in untreated samples, while providing a less variable C:N atomic ratio of 3.06-secular decrease in $\delta^{13}C$ while producing the least variable C:N range of 3.18–3.43. No treatments were able to completely remove the ^{15}N-enriched skin components, with values still increasing to 1–2 ‰ above initial values over time, even under LE/R.

As no standard $C{:}N_{Atomic}$ range has been established for preserved

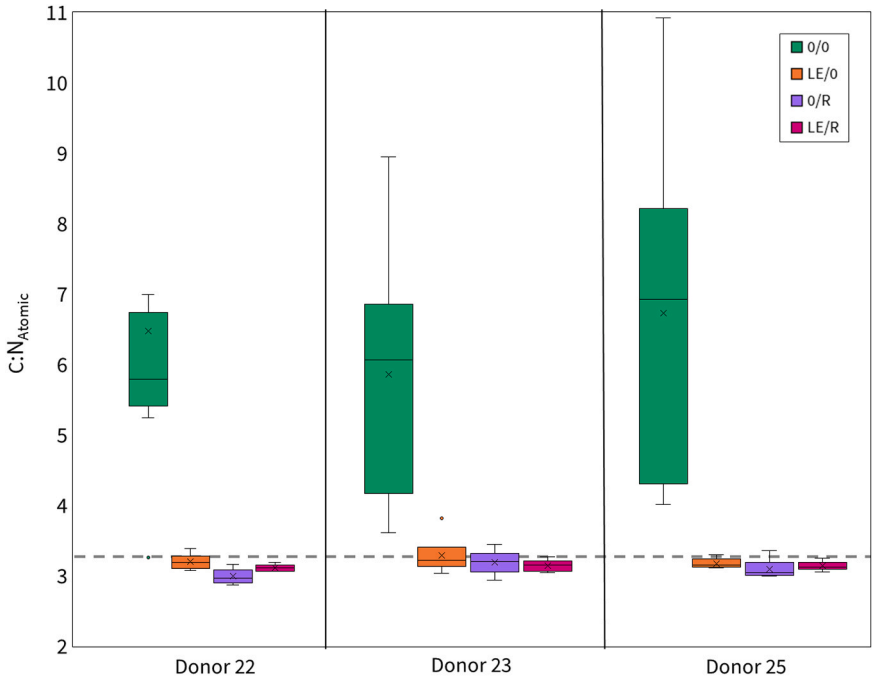

Fig. 6. Visualization of the range of atomic C:N ratios produced from individual-specific skin collected from $n = 3$ donors situated in the RESTES body farm. Untreated samples display significantly higher and more variable atomic C:N ratios than their pretreated counterparts (LE/0: $z = 5.40$, 0/R: $z = 8.34$, LE/R: $z = 7.08$, $p < 0.001$ for all combinations). LE/0 and 0/R differed significantly from each other, but did not differ from LE/R C:N ratios.

skin as this time, comparative assessment of unmodified and decomposition-altered C:N ratios of skin cannot identify differences to the same degree as that applied to the C:N ratios of bone collagen. However, analysis of structural proteins can provide insight into expected skin C:N ratios, allowing for interpretation. As established by Guiry and Szpak [52], the expected $C:N_{Atomic}$ ratios for modern purified mammalian collagen lie within the range of 3.00–3.28, with higher C:N ratios indicating the presence of lipids, non-collagenous proteins, and other high C:N contaminants. This range, however, may not be suitable for assessment of skin. Wilson and Szpak [53] demonstrated that the deamination of glutamine and asparagine that occurs during acidification results in the loss of nitrogen ($-NH_2$ groups) but not carbon. While not altering stable isotope composition, this nitrogen loss produced higher C:N ratios depending on the demineralization applied, with acidic conditions inducing deamidation. As no demineralization is required for skin, it is likely that the $C:N_{Atomic}$ ratio produced from purified skin collagen would be lower than that of purified bone collagen extracted with an HCl demineralization step. Higher C:N ratios in skin may also indicate the presence of the structural components of elastin (C:N of 3.6–3.7) and keratin (C:N of 3.63–3.86), both of which display higher C:N ratios than that of pure collagen [54–61].

While our untreated skin samples displayed high C:N ratios (average C:N of 7.23), chemically pretreated skin provided uniformly lower C:N ratios. Samples treated with both lipid extraction and refluxing exhibited the most consistent C:N ratios of all treatments, with values between 3.18 and 3.43. The C:N range produced by our LE/R samples falls within the range of bone collagen, despite the expectation that skin collagen would likely produce a lower C:N range. As our samples were collected from older individuals, we speculate that the C:N range produced may represent a more significant contribution from higher C:N keratin and elastin content in the skin. This result may be attributed to changes in skin collagen associated with aging (reduced collagen production and quality, increased variation of skin density), the destruction of skin components associated with decomposition, or a unique combination of both factors that warrants further investigation [62]. While not all treatments displayed C:N within that of pure collagen, the values of LE/R treated skin remained in the ranges expected of skin with some non-collagenous protein content and below values indicative of lipid contamination. Presently, we maintain that the application of chemical pretreatments improves the purity of postmortem skin samples in comparison to untreated values. The C:N ratio as a quality control measure provides a means for verifying stable isotope results as representative of changes within skin and skin collagen, rather than various compounds accumulated from the surrounding decomposition environment.

Untreated $\delta^{15}N$ values were found to increase by 1.5–5 ‰ as decomposition progressed, consistent with previous research findings. $\delta^{15}N$ values were found to progressively increase until reaching the active decay stage, identified using Megyesi et al.'s [51] TBS method, corroborating trends of increase in $\delta^{15}N$ identified in previous fish, mammalian, and human studies [27,29,30,32,33,34]. Skin exhibited greater increases in $\delta^{15}N$ in comparison to untreated muscle in another human decomposition study (increase of 1–3 ‰; Beasley et al. [33]). The degree of increase of $\delta^{15}N$ in skin was less robust under colder temperatures, with significant differences identified between the early and late summer donors. Donors placed in early summer exhibited a higher maximum $\delta^{15}N$ of 4–5 ‰ above initial values during the active phase. In comparison, Donor 25, deposited in late summer/early fall, reached only 1.5 ‰ above initial values. Our findings indicate temperature, which significantly influences the pace of decomposition, also concurrently influences the intensity of enriched ^{15}N content in the skin.

In a practical forensic context, it is highly improbable that temporally sequential samples could be collected and analyzed in a similar manner to the methodology applied in this study. However, the comparison of altered $\delta^{15}N$ values of postmortem skin with unaltered, representative $\delta^{15}N$ values produced from bone or hair may provide a practical means to establish time since death, while eliminating the need for multiple, interspersed samples. Similar assessments between sampling materials have previously made between the $\delta^{13}C$ and $\delta^{15}N$ values of hair, bone, and nail for humans, where consideration of material-dependent differences in isotopic values allows for comparison [63]. While temporal variation in diet may complicate the comparison of slower and faster turnover rate materials (such as bone compared to skin), the risk of substantial diet-driven isotopic variation is mitigated by the isotopic homogeneity of the modern industrialized diet [64–66]. The difference between altered (i.e., from skin) and unaltered (i.e., from bone or hair) $\delta^{15}N$ values would therefore reflect the degree of environmental exposure and intensity of temperature. Future examinations of the ^{15}N enrichment of postmortem tissues would benefit from consideration of all environmental variables possible including climate, temperature, humidity, and other elements that may impact the rate of decomposition and isotopic enrichment. Furthermore, the assessment of other isotopic markers, particularly δ^2H, may yield complimentary insight regarding decomposition and merit further research.

During the active decomposition stage, untreated $\delta^{15}N$ was observed to decrease by 0.90–2.45 ‰ occurring within 14–222 days following maximum values. While we were limited in our ability to collect late-stage samples, we suggest that the decline in $\delta^{15}N$ values coincides with the gradual desiccation and mummification of donor skin in the advanced decay stage. TBS under Megyesi et al. [51] identifies the progression of decomposition shifting from moist, active decomposition towards a mummified state. As previously identified by Maisonhaute and Forbes [44], previous human donors exposed to the Quebec climate environment in the REST[ES] facility were found to exhibit prominent desiccation of skin. Displaying dry, parchment-like qualities (terminology following Conner et al. [67]), desiccated skin was found to survive winter exposure and persist on three of four donors beyond the duration of their placement. We propose that the reduced intensity of decomposition processes, paired with the breakdown and expulsion of decomposition products, is reflected as a gradual decrease of $\delta^{15}N$ in desiccated skin. Winter conditions are known to slow and alter decomposition processes, while also resulting in more rapid desiccation [68,69]. Desiccated skin is strongly associated with a decline in decomposition activity, the lack of moisture impeding insect feeding and hydrolytic enzyme processes, including proteolysis [70,71]. As desiccation of skin facilitates less decomposition, processes associated with depletion and enrichment likely become outpaced by the expulsion/evaporation of decomposition byproducts, reflected by decreasing $\delta^{15}N$ values in the skin. Performing closer examination and more thorough sampling transitions between active, advanced, and skeletonized stages and their relationships would provide further insight. Once verified, a reliable increase-decrease pattern in skin $\delta^{15}N$, paired with sequential chemical pretreatments, may provide a foundation for postmortem interval estimation.

The application of different chemical pretreatments was found to provide a new means of examining decomposition and isotopic changes in skin. Lipid extraction was found to reduce the extent of decrease in $\delta^{13}C$ and increase in $\delta^{15}N$, while providing an improved C:N ratio. The $\delta^{15}N$ results are unexpected, as lipid extraction, while effective for removing fats and oils that can create considerable noise in $\delta^{13}C$ values when present in variable quantities, does not significantly impact $\delta^{15}N$ values in bone collagen [72]. A consideration of decomposition chemistry and microbial nitrogen cycling provides a conceptual model of elemental breakdown, isotopic change, and the products removed by different chemical pretreatments.

As decomposition progresses, proteins are broken down through the process of proteolysis. The enzyme protease, produced and introduced by microbial activity, facilitates the breakdown of peptide bonds through hydrolysis [39,73,74]. Amino acids, made accessible through hydrolysis, are subjected to further degradation through one of two series of enzymatic reactions involving oxidation or a combination of oxidation and decarboxylation [39]. In the presence of oxygen, free

amino acids are subjected to an oxidation reaction, facilitated by endogenous or microbe-introduced oxidase [39]. The introduction of oxygen through oxidation produces two products: carboxylic acid and ammonia (NH_3) released from the amino acid structure (Fig. 7A).

Alternatively, free amino acids can also undergo a decarboxylation reaction, facilitated by microbe-introduced decarboxylase (Fig. 7B) [39,74,75], resulting in the formation of one biogenic amine [39,74,75]. Amine byproducts, such as putrescine and cadaverine, can be further broken down through oxidation to produce an aldehyde, while releasing ammonia content from the amino acid into the decomposition environment [39,75,76].

As decomposition progresses, a significant amount of ammonia is produced through the degradation of amino acids, which is then subjected to processes associated with nitrogen cycling, outlined in Fig. 7C. While some ammonia content undergoes volatilization, evaporating into the surrounding environment, exposure to water and acids in the environment facilitates the conversion of ammonia (NH_3) to ammonium (NH_4^+) [74,77]. The microbial process of aerobic nitrification results in the production of nitrite (NO_2^-) which is quickly converted to nitrate (NO_3^-) through oxidation [78]. During anaerobic denitrification, nitrate is converted into nitrite, which is further reduced into nitrogen gas (N_2) and nitrous oxide (N_2O), which are then released into the environment [74].

Microbes have been found to display increased values of $\delta^{15}N$ following the processing of amino acids in both tissue and soil [79–81]. Microbes preferentially convert ^{14}N components into nitrogen gas and nitrous oxide, resulting in the enrichment of ^{15}N in the remaining nitrate [78]. In soil environments, microbial activity induces the accumulation of ^{15}N through fractionation of organic components, where ^{14}N is preferentially processed and released [40,78,82–84]. Ammonia that is relatively depleted of ^{15}N is therefore dispelled through microbial processes, resulting in an accumulation of ammonium (and therefore nitrate) that exhibits higher $\delta^{15}N$ values than the initial organic matter [78]. While the nitrification process involves significant instantaneous fractionation, complete reactions ensure that nitrification often does not impact $\delta^{15}N$ values (i.e., no net fractionation), while anaerobic denitrification facilitates further release of ^{14}N through the production of nitrous oxide.

We propose that the progressive increases in $\delta^{15}N$ observed within our samples are products of the breakdown of proteins facilitated by insect and microbial activity. As amino acids are broken down, we suggest that microbial processing of released ammonia results in the preferential release of ^{14}N, resulting in the accumulation of ^{15}N within the remaining organic compounds. As nitrate is soluble in methanol, nitrate accumulated during decomposition is dissolved by the 2:1 chloroform:methanol treatment applied during lipid extraction. As lipids contain little to no nitrogen, $\delta^{15}N$, wt% N and atomic C:N of material removed during the lipid extraction step would likely reflect the nitrogenous decomposition compounds removed [85]. Further investigation into the isolation of ^{15}N-rich proteolytic byproducts through lipid extraction may provide a new means to examine decomposition over time, accumulated with potential use in determination of the postmortem interval.

Refluxing alone was found to variably improve $\delta^{13}C$, while also displaying robust values of $\delta^{15}N$ of skin, similar to those observed in untreated samples. The 0/R samples displayed values of $\delta^{13}C$ similar yet subtly different to those observed in lipid extracted samples, and in some cases, displayed a lower atomic C:N ratio than those observed in LE inclusive treatments. This implies that the removal of ^{13}C-depleted material from the skin can occur in some capacity during the refluxing step. During decomposition, the enzyme lipase promotes the hydrolysis of triglycerol into components of glycerol, as well as a combination of saturated and unsaturated fatty acids [74,86]. Byproducts of ketones and aldehydes generated from unsaturated fatty acids under aerobic conditions are not found to be soluble in polar solvents such as HCl; as such, these components would be discarded following the refluxing process as insoluble waste. Anaerobic conditions instead facilitate the production of various volatile acids (butyric, valeric, propionic acid), which are soluble in both water and HCl [74,86]. Despite direct exposure to the depositional environment, anaerobic processes can still occur within exposed tissues [77]. The rapid processing of remains by aerobic bacteria has been found to deplete tissues of oxygen, creating optimal conditions for anaerobic bacteria to process the carbon- and hydrogen-rich lipids [77]. As such, anaerobic production of lipid-based acids can occur, which would be promptly dissolved in HCl through the refluxing treatment. Additional acids (citric, glucuronic, oxalic, butyric, acetic, lactic acid) may be produced through the aerobic or anaerobic decomposition of carbohydrates and glucose, which are also soluble in HCl [74]. As acidic byproducts of lipid breakdown are not removed through refluxing, this may explain how refluxing variably improved skin $\delta^{13}C$ values and $C:N_{Atomic}$ in 0/R samples, but not to the degree of lipid extraction-inclusive treatments. Additionally, while the refluxing

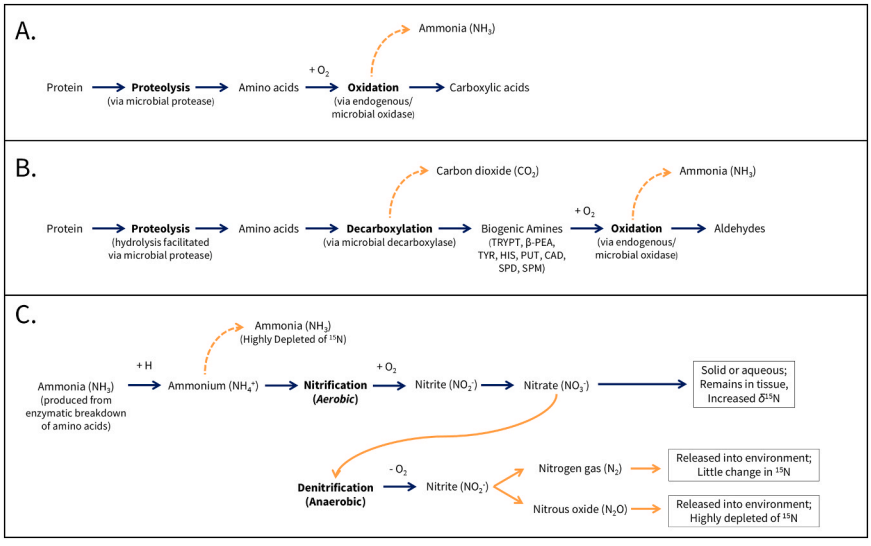

Fig. 7. Visualization of decomposition chemistry associated with protein breakdown, ammonia formation and nitrogen cycling in a decomposition setting, adapted from Sato *et al.* [39] and Ioan *et al.* [74]. A) Oxidation reactions promote the release of amino acid-bound ammonia and the production of carboxylic acids during decomposition. B) Decarboxylation reactions produce decomposition-associated biogenic amines that, once oxidized, releases ammonia and produce an aldehyde. C) Visualization of the processing of ammonia and the mechanisms of nitrogen cycling and enrichment within a decomposition environment.

process likely removes non-collagenous proteins that may alter skin $\delta^{15}N$ values, as decomposition-associated compounds of nitrite and nitrate are not soluble in HCl, we speculate that these ^{15}N-rich compounds are inconsistently preserved during the refluxing process. The 0/R samples displayed both higher $\delta^{15}N$ than the untreated counterparts, as well as more variable $\delta^{13}C$, $\delta^{15}N$ and C:N ratios than the LE treated samples. Therefore, we assert that refluxing alone is unsuitable for the interpretation of skin-bound collagen as well as decomposition, introducing further variability that inhibits both forensic and ecological assessment.

One sample (27972) collected from Donor 22 during the active decay stage exhibited uniquely extreme values of $\delta^{13}C$ (–25.01), $\delta^{15}N$ (+25.11), and $C:N_{Atomic}$ (21.11) not representative of skin, proteins that occur in skin, or lipid-contaminated skin. Following refluxing, three runs of the sample yielded an average atomic C:N ratio of 1.63 (C:N ratios of 1.64, 1.64 and 1.6), well below those expected for collagen and other skin components. Comprised of two amine groups and 4–5 carbon atoms, putrescine ($C_4H_{12}N_2$) and cadaverine ($C_5H_{14}N_2$) exhibit C:N ratios lower than those seen in skin, exhibiting C:N ratios of 2 and 2.5, respectively [87]. As remains decompose, processes of enzymatic decarboxylation and proteolysis can result in the production of putrescine and cadaverine from the amino acids arginine and lysine, detectable throughout the active decomposition stage [88,89]. Both arginine and lysine are essential for the structure and production of collagen, with lysine additionally impacting elastin formation [90,91]. Sampling timing paired with low C:N ratios suggests that this sample is representative of high concentrations of putrescine and cadaverine, extracted during the refluxing step. Within fisheries, amines of putrescine and cadaverine are often measured to determine the suitability of fish for human consumption. Richard *et al.* [92] found that a combination of methanol and HCl was able to consistently extract large amounts of putrescine and cadaverine from fish tissues. This is reflected in the results of the LE/R treatment, with the outlier sample producing values of $\delta^{13}C$ (–20.02), $\delta^{15}N$ (+14.43) and $C:N_{Atomic}$ (3.46) that is, while still distinct, more comparable to other LE/R sample values. Investigating the visualization of biogenic amines through regular and compound-specific stable isotope analysis may provide a more precise means for measuring decomposition progress.

Our findings suggest that the release of amino acid-bound sulfur from reactions of desulfhydration, and processes related to the eventual production of sulfuric acid (H_2SO_4) do not alter $\delta^{34}S$ values [18,74]. As our testing was limited by sample size, we are hesitant to make strong claims regarding changes in $\delta^{34}S$ but these do represent the first sulfur isotopic and elemental data for decomposing human tissues. No trends in $\delta^{34}S$ values were identified over the course of decomposition within our samples, and lipid-extracted skin did not differ significantly from untreated $\delta^{34}S$ values. Donor to donor comparisons indicated significant differences in $\delta^{34}S$, likely reflecting variation in diet [93]. A lack of variation throughout decomposition, and across various pretreatments would bode well for further forensic-oriented stable isotope work that seeks to use $\delta^{34}S$ to assess probable geographic origin, such as humanitarian forensic efforts [93,94].

Untreated skin $\delta^{13}C$ was found to display no consistent increase or decrease over time. Under LE/0 and 0/R treatments, non-significant decreases in $\delta^{13}C$ by up to ~2 ‰ were found to occur within the donors, contrasting the findings of other decomposition studies that identified an increase or no change in tissue $\delta^{13}C$ [27–29]. Cloyed et al. [30] identified decreased $\delta^{13}C$ values in dolphin skin; however, this was interpreted as reflecting their environment rather than as a product of decomposition. Miles [34] provides the only current comparison of lipid-extracted human skin $\delta^{13}C$ values, which identified decreases in the $\delta^{13}C$ values of only 3 of 9 donors.

We recommend the combination of lipid extraction and refluxing for studies looking to examine postmortem tissues when the goal is to determine the isotopic composition of the tissue that reflects the state of the living organism, such as in ecological studies [95]. Untreated, heterogeneous postmortem samples feature lower $\delta^{13}C$ values driven by lipid content, progressively enriched in ^{15}N by decomposition byproducts, and variable C:N ratios. The application of lipid extraction alone was found to consistently improve sample homogeneity, surpassed only by the LE/R treatment, while 0/R treatment was found to be unsuitable for assessment, incompletely removing contaminants and introducing variability. It may be argued that the LE/0 treatment would be most suitable for the analysis of forensically significant tissues, as it produces consistent results while minimizing sample processing and handling. However, under LE/R treatment, decomposition samples were found to exhibit the smallest, most concise range of C:N ratios, indicating that the produced collagen is objectively more "pure". The $\delta^{13}C$ values of human skin within a C:N ratio of 3.18–3.35 were found to exhibit ±1 ‰ variability from both initial and subsequent samples, suggesting that LE/R can produce acceptably pure collagen and $\delta^{13}C$ values from postmortem tissues that are representative of living tissues. $\delta^{15}N$ values in postmortem skin were found to exhibit increases over time, reaching up to 2 ‰ above initial values despite LE/R treatment. This suggests that decomposition processes and their products cannot be completely removed from the skin, even within a homogenous sample produced under LE/R. Therefore, we echo the sentiment of Keenan and DeBruyn [32] that postmortem tissue $\delta^{15}N$ values should be approached with caution and not be interpreted as representative of living tissue values. The analysis of individual compounds (e.g., by GC/C-IRMS or LC-IRMS), or comparable compounds with similar characteristics, when extracted by chemical pre-treatments, may offer a means to more completely trace the impact of decomposition on the isotopic composition of skin.

5. Conclusion

Our isotopic and elemental analysis of postmortem human skin provided new insight into skin $\delta^{13}C$, $\delta^{15}N$ and $\delta^{34}S$ values, and their interactions in a decomposition context. The application of commonly applied sample treatments of lipid extraction and refluxing were found to selectively reveal, remove, and/or emphasize different aspects of decomposition-related modifications identified through stable isotope analysis. These treatments, when applied exclusively or jointly, provided new avenues of visualizing and isolating drivers of postmortem changes in $\delta^{13}C$ and $\delta^{15}N$.

While we are currently unable to establish a method of postmortem interval determination, our findings have broadened our understanding of how stable isotope values of $\delta^{13}C$, $\delta^{15}N$ and $\delta^{34}S$ interact with temperature, decay stage, and decomposition overall. As we continue to examine the relationships between isotope systems and postmortem processes, our efforts should shift to explore new avenues of quantifying decomposition-driven isotopic change, while comprehending the underlying biological mechanisms driving said change. Holistic reporting of research findings, including all donor, stable isotope, and temperature data is a necessity, as limited access to human cadavers is a significant obstacle to the study of decomposition. Continued examination of decomposition processes, paired with analyses from a variety of tissues, contexts, and climates, will help build a foundation for understanding decomposition through stable isotope analysis.

CRediT authorship contribution statement

Ryan Pawlowski: Writing – review & editing, Writing – original draft, Visualization, Methodology, Investigation, Formal analysis, Data curation, Conceptualization. **Forbes Shari L:** Writing – review & editing, Conceptualization. **Paul Szpak:** Writing – review & editing, Supervision, Methodology, Funding acquisition, Conceptualization.

Funding Sources

This work was supported by the Natural Sciences and Engineering Research Council of Canada (NSERC) Research Tools and Instruments Grant [NSERC RTI-2023-00124] and Discovery Horizons Grant [DH-

2022-00198].

Declaration of Competing Interest

The authors declare that they have no known competing financial interests or personal relationships that could have appeared to influence the work reported in this paper.

Acknowledgements

The authors would like to recognize Dr. Matt Teeter for his technical assistance. Additionally, the authors recognize Jerika Ho, Irina Badell, Colin Fraser and Lesley Hewett for assisting with sample collection.

Appendix A. Supporting information

Supplementary data associated with this article can be found in the online version at doi:10.1016/j.forsciint.2026.112871.

References

[1] T. Simmons, Post-mortem interval estimation: an overview of techniques. Taphonomy of Human Remains: Forensic Analysis of the Dead and the Depositional Environment, John Wiley & Sons, Ltd, 2017, pp. 134–142, https://doi.org/10.1002/9781118953358.ch10.
[2] S. Warther, S. Sehner, T. Raupach, K. Püschel, S. Anders, Estimation of the time since death: post-mortem contractions of human skeletal muscles following mechanical stimulation (idiomuscular contraction), Int. J. Leg. Med. 126 (2012) 399–405, https://doi.org/10.1007/s00414-011-0665-3.
[3] T.O. Rognum, S. Holmen, M.A. Musse, P.S. Dahlberg, A. Stray-Pedersen, O. D. Saugstad, S.H. Opdal, Estimation of time since death by vitreous humor hypoxanthine, potassium, and ambient temperature, Forensic Sci. Int. 262 (2016) 160–165, https://doi.org/10.1016/j.forsciint.2016.03.001.
[4] H.T. Gelderman, C.A. Kruiver, R.J. Oostra, M.P. Zeegers, W.L.J.M. Duijst, Estimation of the postmortem interval based on the human decomposition process, J. Forensic Leg. Med. 61 (2019) 122–127, https://doi.org/10.1016/j.jflm.2018.12.004.
[5] J.L. Ruiz López, M. Partido Navadijo, Estimation of the *post-mortem* interval: a review, Forensic Sci. Int. 369 (2025) 112412, https://doi.org/10.1016/j.forsciint.2025.112412.
[6] A.A. Vass, The elusive universal post-mortem interval formula, Forensic Sci. Int. 204 (2011) 34–40, https://doi.org/10.1016/j.forsciint.2010.04.052.
[7] M.A. Iqbal, Maiken Ueland, S.L. Forbes, Recent advances in the estimation of post-mortem interval in forensic taphonomy, Aust. J. Forensic Sci. 52 (2020) 107–123, https://doi.org/10.1080/00450618.2018.1459840.
[8] L. Franceschetti, A. Amadasi, V. Bugelli, G. Bolsi, M. Tsokos, Estimation of late postmortem interval: where do we stand? A literature review, Biology 12 (2023) 783, https://doi.org/10.3390/biology12060783.
[9] M.J. Buchan, G.S. Anderson, Time since death: a review of the current status of methods used in the later postmortem interval, Can. Soc. Forensic Sci. J. 34 (2001) 1–22, https://doi.org/10.1080/00085030.2001.10757514.
[10] A.E. Maile, C.G. Inoue, L.E. Barksdale, D.O. Carter, Toward a universal equation to estimate postmortem interval, Forensic Sci. Int. 272 (2017) 150–153, https://doi.org/10.1016/j.forsciint.2017.01.013.
[11] M. Caccianiga, G. Caccia, D. Mazzarelli, D. Salsarola, P. Poppa, D. Gaudio, A. Cappella, L. Franceschetti, S. Tambuzzi, L. Maggioni, C. Cattaneo, Common and much less common scenarios in which botany is crucial for forensic pathologist and anthropologists: a series of eight case studies, Int. J. Leg. Med. 135 (2021) 1067–1077, https://doi.org/10.1007/s00414-020-02456-0.
[12] B. Beard, C. Johnson, Strontium isotope composition of skeletal material can determine the birth place and geographic mobility of humans and animals, J. Forensic Sci. 45 (2000) 1049–1061, https://doi.org/10.1520/JFS14829J.
[13] J. Aggarwal, J. Habicht-Mauche, C. Juarez, Application of heavy stable isotopes in forensic isotope geochemistry: a review, Appl. Geochem. 23 (2008) 2658–2666, https://doi.org/10.1016/j.apgeochem.2008.05.016.
[14] W. Meier-Augenstein, I. Fraser, Forensic isotope analysis leads to identification of a mutilated murder victim, Sci. Justice 48 (2008) 153–159, https://doi.org/10.1016/j.scijus.2007.10.010.
[15] L.A. Chesson, G.E. Berg, The use of stable isotopes in postconflict forensic identification, WIREs Forensic Sci. 4 (2022) e1439, https://doi.org/10.1002/wfs2.1439.
[16] S. Ammer, R. Kramer, E. Bartelink, Chapter 9 - forensic isotope provenancing for undocumented border crosser human remains: application, overview, and case studies, in, in: A.H. Ross, J.H. Byrd (Eds.), Methodological and Technological Advances in Death Investigations, Academic Press, 2024, pp. 259–301, https://doi.org/10.1016/B978-0-12-819394-5.00013-4.
[17] H.K. Graham, A. Eckersley, M. Ozols, K.T. Mellody, M.J. Sherratt, Human skin: composition, structure and visualisation methods, in: G. Limbert (Ed.), From Experimental Characterisation to Advanced Modelling, Skin Biophysics, Springer International Publishing, Cham, 2019, pp. 1–18, https://doi.org/10.1007/978-3-030-13279-8_1.
[18] S.L. Forbes, Decomposition chemistry in a burial environment, CRC Press, 2008, pp. 215–236.
[19] S.L. Forbes, K.A. Perrault, J.L. Comstock, Microscopic post-mortem changes: the chemistry of decomposition. Taphonomy of Human Remains: Forensic Analysis of the Dead and the Depositional Environment, John Wiley & Sons, Ltd, 2017, pp. 26–38, https://doi.org/10.1002/9781118953358.ch2.
[20] S.K. Todd, B. Holm, D.A.S. Rosen, D.J. Tollit, Stable isotope signal homogeneity and differences between and within pinniped muscle and skin, Mar. Mammal. Sci. 26 (2009) 176–185, https://doi.org/10.1111/j.1748-7692.2009.00345.x.
[21] M. Arregui, M. Josa, A. Aguilar, A. Borrell, Isotopic homogeneity throughout the skin in small cetaceans, Rapid Commun. Mass Spectrom. 31 (2017) 1551–1557, https://doi.org/10.1002/rcm.7936.
[22] A. Borrell, P. Sant, G. Víkingsson, A. Aguilar, R. García-Vernet, An evaluation of whale skin differences and its suitability as a tissue for stable isotope analysis, J. Sea Res. 140 (2018) 59–62, https://doi.org/10.1016/j.seares.2018.07.011.
[23] A.A.Y. Derian, R. Pawlowski, P. Szpak, Solubilization of skin collagen improves the accuracy and reliability of stable isotope measurements, PeerJ 13 (2025) e20152, https://doi.org/10.7717/peerj.20152.
[24] K.M. Halprin, Epidermal "turnover time"—a re-examination, Br. J. Dermatol. 86 (1972) 14–19, https://doi.org/10.1111/j.1365-2133.1972.tb01886.x.
[25] M.I. Koster, Making an epidermis, Ann. N. Y Acad. Sci. 1170 (2009) 7–10, https://doi.org/10.1111/j.1749-6632.2009.04363.x.
[26] A.L. Lamb, Stable isotope analysis of soft tissues from mummified human remains, Environ. Archaeol. 21 (2016) 271–284, https://doi.org/10.1080/14614103.2015.1101937.
[27] A. Payo-Payo, B. Ruiz, L. Cardona, A. Borrell, Effect of tissue decomposition on stable isotope signatures of striped dolphins Stenella coeruleoalba and loggerhead sea turtles Caretta caretta, Aquat. Biol. 18 (2013) 141–147, https://doi.org/10.3354/ab00497.
[28] D.J. Yurkowski, A.J. Hussey, N.E. Hussey, A.T. Fisk, Effects of decomposition on carbon and nitrogen stable isotope values of muscle tissue of varying lipid content from three aquatic vertebrate species, Rapid Commun. Mass Spectrom. 31 (2017) 389–395, https://doi.org/10.1002/rcm.7802.
[29] M.J. Perkins, Y.K.Y. Mak, L.S.R. Tao, A.T.L. Wong, J.K.C. Yau, D.M. Baker, K.M. Y. Leung, Short-term tissue decomposition alters stable isotope values and C:N ratio, but does not change relationships between lipid content, C:N ratio, and Δδ13C in marine animals, PLOS One 13 (2018) e0199680, https://doi.org/10.1371/journal.pone.0199680.
[30] C.S. Cloyed, C. Johnson, K.P. DaCosta, L.R. Clance, M.L. Russell, C. Díaz Clark, E. E. Hieb, R.H. Carmichael, Effects of tissue decomposition on stable isotope ratios and implications for use of stranded animals in research, Ecosphere 14 (2023) e4385, https://doi.org/10.1002/ecs2.4385.
[31] J.L. McHugh, The whale problem: a status report a book review and perspective, Ocean Dev. Int. Law 3 (1976) 389–411, https://doi.org/10.1080/00908327509545576.
[32] S.W. Keenan, J.M. DeBruyn, Changes to vertebrate tissue stable isotope (δ15N) composition during decomposition, Sci. Rep. 9 (2019) 9929, https://doi.org/10.1038/s41598-019-46368-5.
[33] M. Beasley, J. Lesnik, H. McKee-Zech, A. Duncan, Using stable nitrogen isotope ratios from human skeletal muscle tissue for postmortem interval (PMI) Estimation (Part 1), FA (2024), https://doi.org/10.5744/fa.2023.0001.
[34] Kelly Miles, Forensic taphonomy and stable isotopes: an examination of δ13C and δ15. N in decomposing skin, muscle, and grave soil as an indicator of post mortem interval, Univesity of New Brunswick, PhD. dissertation, 2023.
[35] R. Longin, New method of collagen extraction for radiocarbon dating, Nature 230 (1971) 241–242, https://doi.org/10.1038/230241a0.
[36] E.G. Bligh, W.J. Dyer, A rapid method of total lipid extraction and purification, Can. J. Biochem. Physiol. 37 (1959) 911–917, https://doi.org/10.1139/o59-099.
[37] E.J. Guiry, P. Szpak, Quality control for modern bone collagen stable carbon and nitrogen isotope measurements, Methods Ecol. Evol. 11 (2020) 1049–1060, https://doi.org/10.1111/2041-210X.13433.
[38] Q. Yu, R. Zhou, Y. Wang, W. Su, J. Yang, T. Feng, Y. Dou, H. Li, Carcass decay deteriorates water quality and modifies the *nirS* denitrifying communities in different degradation stages, Sci. Total Environ. 785 (2021) 147185, https://doi.org/10.1016/j.scitotenv.2021.147185.
[39] H. Sato, T. Umehara, S. Kimura, T. Tanaka, S.-E. Kim, Determination of putrefactive amine and ammonia concentrations around decomposed corpses, J. Toxicol. Sci. 50 (2025) 75–81, https://doi.org/10.2131/jts.50.75.
[40] S.W. Keenan, S.M. Schaeffer, J.M. DeBruyn, Spatial changes in soil stable isotopic composition in response to carrion decomposition, Biogeosciences 16 (2019) 3929–3939, https://doi.org/10.5194/bg-16-3929-2019.
[41] J. Folch, M. Lees, G.H.S. Stanley, A simple method for the isolation and purification of total lipides from animal tissues, J. Biol. Chem. 226 (1957) 497–509, https://doi.org/10.1016/S0021-9258(18)64849-5.
[42] D.M. Post, C.A. Layman, D.A. Arrington, G. Takimoto, J. Quattrochi, C.G. Montaña, Getting to the fat of the matter: models, methods and assumptions for dealing with lipids in stable isotope analyses, Oecologia 152 (2007) 179–189, https://doi.org/10.1007/s00442-006-0630-x.
[43] T.A. Brown, D.E. Nelson, J.S. Vogel, J.R. Southon, Improved collagen extraction by modified longin method, Radiocarbon 30 (1988) 171–177, https://doi.org/10.1017/S0033822200044118.
[44] E.L. Pecsi, G. Bronchti, F. Crispino, S.L. Forbes, Perspectives on the establishment of a canadian human taphonomic facility: the experience of REST[ES], Forensic

Science International Synergy 2 (2020) 287–292, https://doi.org/10.1016/j.fsisyn.2020.09.001.
[45] J.-É. Maisonhaute, S.L. Forbes, Decomposition process and arthropod succession on pig carcasses in Quebec (Canada), Can. Soc. Forensic Sci. J. 54 (2021) 1–26, https://doi.org/10.1080/00085030.2020.1820799.
[46] P. Szpak, K. Krippner, M.P. Richards, Effects of sodium hydroxide treatment and ultrafiltration on the removal of humic contaminants from archaeological bone, Int. J. Osteoarchaeol. 27 (2017) 1070–1077, https://doi.org/10.1002/oa.2630.
[47] B.C. Finucane, Mummies, maize, and manure: multi-tissue stable isotope analysis of late prehistoric human remains from the Ayacucho Valley, Perú, J. Archaeol. Sci. 34 (2007) 2115–2124, https://doi.org/10.1016/j.jas.2007.02.006.
[48] F. Fourel, F. Martineau, M. Seris, C. Lécuyer, Simultaneous N, C, S stable isotope analyses using a new purge and trap elemental analyzer and an isotope ratio mass spectrometer, Rapid Commun. Mass Spectrom. 28 (2014) 2587–2594, https://doi.org/10.1002/rcm.7048.
[49] P. Szpak, An automated spreadsheet for determining analytical uncertainty of stable isotope measurements, J. Archaeol. Sci. (2026), https://doi.org/10.2139/ssrn.5404346.
[50] O. Hammer, D.A.T. Harper, P.D. Ryan, Paleontological Statistics Software Package for Education and Data Analysis (2001).
[51] M. Megyesi, S. Nawrocki, N. Haskell, Using accumulated degree-days to estimate the postmortem interval from decomposed human remains, J. Forensic Sci. 50 (2005) 1–9, https://doi.org/10.1520/JFS2004017.
[52] E.J. Guiry, P. Szpak, Quality control for modern bone collagen stable carbon and nitrogen isotope measurements, Methods Ecol. Evol. 11 (2020) 1049–1060, https://doi.org/10.1111/2041-210X.13433.
[53] T. Wilson, P. Szpak, Acidification does not alter the stable isotope composition of bone collagen, PeerJ 10 (2022) e13593, https://doi.org/10.7717/peerj.13593.
[54] S. Rothberg, R.G. Crounse, L. Davis, L. Avogardo, J. Lamas, The Amino Acid Composition of Protein Fractions from Normal and Abnormal Epidermis**From the Dermatology Branch, National Cancer Institute, National Institutes of Health, Public Health Service, U.S. Department of Health, Education and Welfare, Bethesda, Maryland and the Department of Dermatology, University of Miami School of Medicine, Miami, Florida, J. Invest. Dermatol. 44 (1965) 320–325, https://doi.org/10.1038/jid.1965.56.
[55] H. Lindley, The chemical composition and structure of wool, in: R.S. Asquith (Ed.), Chemistry of Natural Protein Fibers, Springer US, Boston, MA, 1977, pp. 147–191, https://doi.org/10.1007/978-1-4613-4109-3_4.
[56] T. Miyahara, S. Shiozawa, A. Murai, The effect of age on amino acid composition of human skin collagen, J. Gerontol. 33 (1978) 498–503, https://doi.org/10.1093/geronj/33.4.498.
[57] T. Samata, M. Matsuda, Studies on the amino acid compositions of the equine body hair and the hoof, Jpn. J. Vet. Sci. 50 (1988) 333–340, https://doi.org/10.1292/jvms1939.50.333.
[58] J.M. Gillespie, The proteins of hair and other hard α-Keratins, in: R.D. Goldman, P. M. Steinert (Eds.), Cellular and Molecular Biology of Intermediate Filaments, Springer US, Boston, MA, 1990, pp. 95–128, https://doi.org/10.1007/978-1-4757-9604-9_4.
[59] J. Yu, D. Yu, D.M. Checkla, I.M. Freedberg, A.P. Bertolino, Human hair keratins, J. Invest. Dermatol. Proc. 41st Annu. Symp Biol. Ski. 101 (1993) S56–S59, https://doi.org/10.1016/0022-202X(93)90501-8.
[60] W.H. Hendriks, M.F. Tarttelin, P.J. Moughan, The amino acid composition of cat (Felis catus) hair, Anim. Sci. 67 (1998) 165–170, https://doi.org/10.1017/S1357729800009905.
[61] E.D. Connolly, G. Wu, Functions and metabolism of amino acids in the hair and skin of dogs and cats, in: G. Wu (Ed.), Nutrition and Metabolism of Dogs and Cats, Springer Nature Switzerland, Cham, 2024, pp. 135–154, https://doi.org/10.1007/978-3-031-54192-6_6.
[62] D.M. Reilly, J. Lozano, Skin collagen through the lifestages: importance for skin health and beauty (2021), https://doi.org/10.20517/2347-9264.2020.153 par 8, N/A-N/A.
[63] T.C. O'Connell, R.E.M. Hedges, Isotopic comparison of hair and bone: archaeological analyses, J. Archaeol. Sci. 26 (1999) 661–665, https://doi.org/10.1006/jasc.1998.0383.
[64] C. Lehn, A. Rossmann, M. Graw, Provenancing of unidentified corpses by stable isotope techniques – presentation of case studies, Sci. Justice 55 (2015) 72–88, https://doi.org/10.1016/j.scijus.2014.10.006.
[65] O. Hall, S. Forbes, P. Szpak, Variation in human bone collagen turnover among skeletal elements, Am. J. Biol. Anthropol 189 (2026), https://doi.org/10.1002/ajpa.70199.
[66] M.I. Bird, S.A. Crabtree, J. Haig, S. Ulm, C.M. Wurster, A global carbon and nitrogen isotope perspective on modern and ancient human diet, Proc. Natl. Acad. Sci. U. S. A. 118 (2021) e2024642118, https://doi.org/10.1073/pnas.2024642118.
[67] M. Connor, C. Baigent, E.S. Hansen, Measuring desiccation using qualitative changes: a step toward determining regional decomposition sequences, J. Forensic Sci. 64 (2019) 1004–1011, https://doi.org/10.1111/1556-4029.14003.
[68] L.E. MacAulay, D.G. Barr, D.B. Strongman, Effects of decomposition on gunshot wound characteristics: under cold temperatures with no insect activity, J. Forensic Sci. 54 (2009) 448–451, https://doi.org/10.1111/j.1556-4029.2008.00980.x.
[69] J. Meyer, B. Anderson, D.O. Carter, Seasonal variation of carcass decomposition and gravesoil chemistry in a cold (Dfa) climate, J. Forensic Sci. 58 (2013) 1175–1182, https://doi.org/10.1111/1556-4029.12169.
[70] D.A. Finaughty, A.G. Morris, Precocious natural mummification in a temperate climate (Western Cape, South Africa), Forensic Sci. Int. 303 (2019) 109948, https://doi.org/10.1016/j.forsciint.2019.109948.
[71] D.O. Carter, D. Yellowlees, M. Tibbett, Moisture can be the dominant environmental parameter governing cadaver decomposition in soil, Forensic Sci. Int. 200 (2010) 60–66, https://doi.org/10.1016/j.forsciint.2010.03.031.
[72] E.J. Guiry, P. Szpak, M.P. Richards, Effects of lipid extraction and ultrafiltration on stable carbon and nitrogen isotopic compositions of fish bone collagen, Rapid Comm. Mass Spectrom. 30 (2016) 1591–1600, https://doi.org/10.1002/rcm.7590.
[73] H. Jakubke, P. Kuhl, A. Könnecke, Basic principles of protease-catalyzed peptide bond formation, Angew. Chem. Int. Ed. Engl. 24 (1985) 85–93, https://doi.org/10.1002/anie.198500851.
[74] B.G. Ioan, C. Manea, B. Hanganu, L. Statescu, L. Gheuca Solovastru, I. Manoilescu, The chemistry decomposition in human corpses, Rev. Chim. 68 (2017) 1352–1356, https://doi.org/10.37358/RC.17.6.5672.
[75] W. Wójcik, M. Łukasiewicz, K. Puppel, Biogenic amines: formation, action and toxicity – a review, J. Sci. Food Agric. 101 (2021) 2634–2640, https://doi.org/10.1002/jsfa.10928.
[76] E.M. Hoffman, A.M. Curran, N. Dulgerian, R.A. Stockham, B.A. Eckenrode, Characterization of the volatile organic compounds present in the headspace of decomposing human remains, Forensic Sci. Int. 186 (2009) 6–13, https://doi.org/10.1016/j.forsciint.2008.12.022.
[77] B.B. Dent, S.L. Forbes, B.H. Stuart, Review of human decomposition processes in soil, Env Geol. 45 (2004) 576–585, https://doi.org/10.1007/s00254-003-0913-z.
[78] S. Deb, D. Lewicka-Szczebak, L. Rohe, Microbial nitrogen transformations tracked by natural abundance isotope studies and microbiological methods: a review, Sci. Total Environ. 926 (2024) 172073, https://doi.org/10.1016/j.scitotenv.2024.172073.
[79] S.A. Macko, M.L.F. Estep, Microbial alteration of stable nitrogen and carbon isotopic compositions of organic matter, Org. Geochem. 6 (1984) 787–790, https://doi.org/10.1016/0146-6380(84)90100-1.
[80] T.Z. Lerch, N. Nunan, M.-F. Dignac, C. Chenu, A. Mariotti, Variations in microbial isotopic fractionation during soil organic matter decomposition, Biogeochemistry 106 (2011) 5–21, https://doi.org/10.1007/s10533-010-9432-7.
[81] S.W. Keenan, S.M. Schaeffer, V.L. Jin, J.M. DeBruyn, Mortality hotspots: Nitrogen cycling in forest soils during vertebrate decomposition, Soil Biol. Biochem. 121 (2018) 165–176, https://doi.org/10.1016/j.soilbio.2018.03.005.
[82] S.L. Connin, X. Feng, R.A. Virginia, Isotopic discrimination during long-term decomposition in an arid land ecosystem, Soil Biol. Biochem. 33 (2001) 41–51, https://doi.org/10.1016/S0038-0717(00)00113-9.
[83] S.A. Billings, D.D. Richter, Changes in stable isotopic signatures of soil nitrogen and carbon during 40 years of forest development, Oecologia 148 (2006) 325–333, https://doi.org/10.1007/s00442-006-0366-7.
[84] J.M. Craine, E.N.J. Brookshire, M.D. Cramer, N.J. Hasselquist, K. Koba, E. Marin-Spiotta, L. Wang, Ecological interpretations of nitrogen isotope ratios of terrestrial plants and soils, Plant Soil 396 (2015) 1–26, https://doi.org/10.1007/s11104-015-2542-1.
[85] J.M. Logan, T.D. Jardine, T.J. Miller, S.E. Bunn, R.A. Cunjak, M.E. Lutcavage, Lipid corrections in carbon and nitrogen stable isotope analyses: comparison of chemical extraction and modelling methods, J. Anim. Ecol. 77 (2008) 838–846.
[86] J. Hayman, M. Oxenham, Chapter 3 - biochemical methods of estimating the time since death, in, in: J. Hayman, M. Oxenham (Eds.), Human Body Decomposition, Academic Press, 2016, pp. 53–90, https://doi.org/10.1016/B978-0-12-803691-4.00003-0.
[87] C. Izquierdo, J.C. Gómez-Tamayo, J.-C. Nebel, L. Pardo, A. Gonzalez, Identifying human diamine sensors for death related putrescine and cadaverine molecules, PLoS Comput. Biol. 14 (2018) e1005945, https://doi.org/10.1371/journal.pcbi.1005945.
[88] S. Paczkowski, S. Schütz, Post-mortem volatiles of vertebrate tissue, Appl. Microbiol Biotechnol. 91 (2011) 917–935, https://doi.org/10.1007/s00253-011-3417-x.
[89] J.Y. Balta, G. Blom, A. Davidson, K. Perrault, J.F. Cryan, S.M. O'Mahony, J. P. Cassella, Developing a quantitative method to assess the decomposition of embalmed human cadavers, Forensic Chem. 18 (2020) 100235, https://doi.org/10.1016/j.forc.2020.100235.
[90] R. Saini, M. Pharm, Ph.D., Z., A, Arginine Derived Nitric Oxide: Key to Healthy Skin (2013) 73–82, https://doi.org/10.1007/978-1-62703-167-7_8.
[91] S.M. Mithieux, A.S. Weiss, Elastin. Advances in Protein Chemistry, Fibrous Proteins: Coiled-Coils, Collagen and Elastomers, Academic Press, 2005, pp. 437–461, https://doi.org/10.1016/S0065-3233(05)70013-9.
[92] N.L. Richard, L.F. Pivarnik, P.C. Ellis, C.M. Lee, Impact of quality parameters on the recovery of putrescine and cadaverine in fish using methanol-hydrochloric acid solvent extraction, J. AOAC Int. 94 (2011) 1177–1188, https://doi.org/10.1093/jaoac/94.4.1177.
[93] S. Ammer, E. Bartelink, J. Vollner, B. Anderson, E. Cunha, Socioeconomic and geographic implications from carbon, nitrogen, and sulfur isotope ratios in human hair from Mexico, Forensic Sci. Int. 316 (2020) 110455, https://doi.org/10.1016/j.forsciint.2020.110455.
[94] E.J. Bartelink, L.A. Chesson, Recent applications of isotope analysis to forensic anthropology, Forensic Sci. Res. 4 (2019) 29–44, https://doi.org/10.1080/20961790.2018.1549527.
[95] R. Ferreira, E. Dias, M. Kaufmann, M. Fernandez, F. Alves, Revealing trophic interactions among sympatric odontocetes in an oceanic ecosystem through stable isotope analysis, J. Zool. (2025) jzo.70053, https://doi.org/10.1111/jzo.70053.